Journal of Biomechanics 165 (2024) 112025

Contents lists available at ScienceDirect

Journal of Biomechanics

journal homepage: www.elsevier.com/locate/jbiomech

Association between fat and fat-free body mass indices on shock attenuation during running

Bernard X.W. Liew [a,*], Xuqi Zhu [b], Xiaojun Zhai [c], Stuart A. McErlain-Naylor [c], Christopher McManus [a]

[a] School of Sport, Rehabilitation and Exercise Sciences, University of Essex, Colchester, Essex, United Kingdom
[b] School of Computer Science and Electrical Engineering, University of Essex, Colchester, Essex, United Kingdom
[c] School of Sport, Exercise and Health Sciences, Loughborough University, Loughborough, United Kingdom

ARTICLE INFO

Keywords:
Body composition
Adiposity
Acceleration
Elastic wave
Tibia

ABSTRACT

High amplitudes of shock during running have been thought to be associated with an increased injury risk. This study aimed to quantify the association between dual-energy X-ray absorptiometry (DEXA) quantified body composition, and shock attenuation across the time and frequency domains. Twenty-four active adults participated. A DEXA scan was performed to quantify the fat and fat-free mass of the whole-body, trunk, dominant leg, and viscera. Linear accelerations at the tibia, pelvis, and head were collected whilst participants ran on a treadmill at a fixed dimensionless speed 1.00 Fr. Shock attenuation indices in the time- and frequency-domain (lower frequencies: 3–8 Hz; higher frequencies: 9–20 Hz) were calculated. Pearson correlation analysis was performed for all combinations of DEXA and attenuation indices. Regularised regression was performed to predict shock attenuation indices using DEXA variables. A greater power attenuation between the head and pelvis within the higher frequency range was associated with a greater trunk fat-free mass ($r = 0.411$, $p = 0.046$), leg fat-free mass ($r = 0.524$, $p = 0.009$), and whole-body fat-free mass ($r = 0.480$, $p = 0.018$). For power attenuation of the high-frequency component between the pelvis and head, the strongest predictor was visceral fat mass ($\beta = 48.79$). Passive and active tissues could represent important anatomical factors aiding in shock attenuation during running. Depending on the type and location of these masses, an increase in mass may benefit injury risk reduction. Also, our findings could implicate the injury risk potential during weight loss programs.

1. Introduction

During running, the body undergoes rapid deceleration when the foot contacts the ground resulting in a shock wave transmitting from the ground, through the body, reaching the head (Chadefaux et al., 2019; Shorten and Winslow, 1992). High amplitudes of shock wave during running have been thought to contribute to the risk of lower-limb injuries (Zadpoor and Nikooyan, 2011), and even contribute to the destabilisation of the visual fields (Busa et al., 2016). In addition to the amplitude of shock, the frequency characteristics of the shock wave may also be important to understand (Shorten and Winslow, 1992). The power of a shock wave at different ranges of frequencies has different sources (Shorten and Winslow, 1992), with different potential for modification strategies to be employed (Gruber et al., 2014). For example, the lower frequency (3–8 Hz) range of a shock wave can be attributed to the active motion of the body segments during running, whilst the higher frequency (9–20 Hz) range reflects the post-impact shock wave (Derrick et al., 1998).

A greater shock attenuation means that the amplitude (time-domain) or the power (frequency-domain) of the shock wave decreases distal to proximally, and. is thought to be beneficial for reducing injury risk potential. The body uses a variety of movement strategies to attenuate the shock transmission across body regions. For example, running with a reduced step length (Baggaley et al., 2020), landing with a greater knee flexion angle (Edwards et al., 2012), and running with a preferred movement strategy (Enders et al., 2014), enable greater shock attenuation. During landing, soft tissue movements play an important role in shock attenuation, although most of the focus has been on the role of active tissues (i.e. muscles) (Pain and Challis, 2002; Pain and Challis, 2006; Wakeling et al., 2003). The role of passive soft tissue structures and their relationship to shock attenuation during running has been an under-investigated area of research. A previous study on obese adults

* Corresponding author.
E-mail address: bl19622@essex.ac.uk (B.X.W. Liew).

https://doi.org/10.1016/j.jbiomech.2024.112025
Accepted 22 February 2024
Available online 24 February 2024

reported that passive soft tissues performed a significant amount of negative work during walking (Fu et al., 2015). Interestingly, another study reported a lower magnitude of distal to proximal shock attenuation in obese children (body mass index [BMI] 24.1 $kg{\cdot}m^{-2}$) compared to non-obese children (BMI 17.4 $kg{\cdot}m^{-2}$) (Tirosh et al., 2020).

A disadvantage of BMI is that it does not provide a quantitative measure of fat mass and its distribution. Conversely, dual-energy X-ray absorptiometry (DEXA) defines the composition of the body as three compartments: bone mineral content, fat mass, and lean body mass. Fat mass encompasses all lipid mass, including triglycerides, phospholipids, and lipids in organ, marrow, and subcutaneous adipose tissues, whereas lipid-free, lean body mass is the sum of all non-bone, non-fat soft tissues in the body, primarily comprising water, protein, soft tissue mineral, and glycogen (IAEA, 2011). One study reported that whole body lean mass and fat mass quantified via dual-energy X-ray absorptiometry (DEXA) were highly correlated (r = 0.8–0.90) with vertical ground reaction force impact peak and loading rate during walking in obese children (Villarrasa-Sapiña et al., 2017). Another study reported that thigh fat had close to 10 times stronger association with knee contact forces than abdominal fat (Messier et al., 2014). Although studies have quantified the relationship between lean and fat mass and peak tibial accelerations (Giandolini et al., 2019), no studies to our knowledge have quantified how fat mass and its distribution are related to regional shock attenuation during running.

The primary aim of this study was to explore whether quantitative measures of body composition via DEXA are associated with shock attenuation across the time and frequency domains during running. We hypothesised that a greater fat mass would be associated with greater shock attenuation and that the association will be strongest when making regional, rather than global, comparisons. We also hypothesised that the greater the whole-body fat mass, the greater the attenuation of whole-body shock across the time and frequency domain. We also hypothesised that a greater fat mass across a specific region would be associated with a greater shock attenuation across the same body regions.

2. Methods

2.1. Participants

This study adopted a cross-section design involving a single testing session. Inclusion criteria were: 1) age 18–40 years; 2) self-reported absence of any medical conditions that would preclude safe completion of submaximal running; 3) absence of lower-limb pain/injury within the previous 3 months; and 4) self-reported ability to run on a treadmill continuously for 20 min. All participants provided signed an electronic informed consent. This study was approved by the University of Essex's Human Research Ethics Committee (ETH2223-0475).

2.2. Sample size

A previous study reported a peak acceleration attenuation coefficient difference of 23.5 % between overweight and non-overweight children who differed in BMI by 6.7 $kg{\cdot}m^{-2}$ (Tirosh et al., 2020). Given a linear relationship between attenuation and BMI, this provides a linear relation of 3.5 (i.e. $\frac{23.5}{6.7}$). Given a standard deviation in the attenuation coefficient of 25 (Tirosh et al., 2020), and BMI of 3, the correlation coefficient linking BMI to the outcome of attenuation will be 0.4 (i.e. $3.5 \times \frac{3}{25}$). To detect a correlation coefficient of 0.4, at a power of 0.8 and an alpha of 0.05, a total of 24 participants will be needed.

2.3. Participant characteristics

Descriptive characteristics of the participants' age, gender, and current running history – running experience (years), maximal running distance in the past three months, and weekly running frequency, were collected (Nielsen et al., 2019).

2.4. Dual-energy X-ray absorptiometry (DEXA)

Height and body mass (Seca, model 770, Germany), measured with participants dressed in light sports clothing with shoes removed, were used to calculate body mass index (BMI). The evaluation of body composition was carried out using a DEXA scan (Hologic Horizon W, Hologic Inc., Marlborough, MA, USA), facilitated by the Hologic APEX software version 5.6.0.5. Participants were advised to follow their regular dietary routine on the day of the scan but were offered the possibility to empty their bladder before the scan. They were allowed to wear either undergarment with a hospital-provided gown or their own sportswear, which could include shorts and a loose-fitting shirt. For the DEXA scan, participants were laid supine along the central longitudinal axis of the DEXA table, arms placed at their sides with palms facing downward. Legs were kept shoulder width apart with hips internally rotated and the feet taped together at the level of the metatarsophalangeal joints to ensure a consistent position throughout the scan (Bilsborough et al., 2014). All scans were manually adjusted by a single DEXA operator to correct the automated partition of body regions, verifying the separation of the arms at the glenohumeral joints and the legs at the acetabulofemoral joints (Nana et al., 2015). Analysis of the DEXA scans were used to quantify whole body, trunk, dominant leg, and visceral fat region measures of total mass (kg), fat mass (kg), and fat-free mass (kg) (Eq. (1)) (Table 1).

$$Fat-free\ mass\ (kg) = Lean\ body\ mass + Bone\ mineral\ content \quad (1)$$

2.5. Running assessment

Participants wore their habitual running shoes. Four inertial measurement units (IMUs, Noraxon Ultium Motion, USA, 400 Hz) were affixed to the dorsum of the foot, medial surface of the distal tibia immediately above the medial malleolus, posterior surface of the sacrum, and frontal portion of the forehead, using elastic straps provided by the manufacturer. The straps were tightened to the limit of the participant's self-reported comfort. The lower-limb sensors were affixed to the self-reported dominant limb (i.e. side used to kick a ball). The foot IMU was used for initial contact and toe-off detection using the manufacturer's proprietary algorithm.

All participants ran on a treadmill (HP Cosmos, C, Quasar LE 500 CE, HP Cosmos, Nussdorf-Traunstein, Germany) at a fixed dimensionless speed 1.00 Fr (Fr = Froude number) (Castillo and Lieberman, 2018), whilst wearing a torso safety harness. Participants completed two minutes of running at the required speed to minimise the effect of fatigue. The middle 30 s of the trial were extracted for subsequent analysis (Castillo and Lieberman, 2018).

Table 1
Exported DEXA variables.

Variables	Manufacturer's descriptor of variables
TRUNK FAT	Grams of Fat tissue in trunk region.
TRUNK LEAN	Grams of Fat-free (lean body mass + bone mineral content) tissue in trunk region.
LEG FAT	Grams of Fat tissue in dominant leg region.
LEG LEAN	Grams of Fat-free (lean body mass + bone mineral content) tissue in dominant leg region.
WBTOT FAT	Total Grams of Fat tissue in all included regions.
WBTOT LEAN	Total Grams of Fat-free (lean body mass + bone mineral content) tissue in all included regions.
VFAT BODY FAT	Fat Tissue in largest Visceral Fat region.
VFAT BODY LEAN	Fat-free tissue in largest Visceral Fat region

2.6. Data processing

Events of initial contact and toe-off were identified using Noraxon's proprietary algorithm based on the foot accelerometer signals and used for segmenting the tri-axial accelerometer signals. The resultant accelerometer signal ($\sqrt{x^2+y^2+z^2}$) for each sensor was calculated and used for all subsequent analyses to account for attenuation across all three dimensions (Sheerin et al., 2019) (Fig. 1).

2.6.1. Time domain analysis

The three-dimensional (3D) accelerometer signals were filtered using a fourth-order, zero-phase digital Butterworth low-pass filter at 60 Hz (Castillo and Lieberman, 2018), prior to calculating the resultant signal. For each stance phase cycle, the peak resultant acceleration magnitude for each sensor was extracted. The shock attenuation index was calculated based on the following formulas (Reenalda et al., 2019):

$$Shockattenuation^{tibial}(\%) = \left[1 - \frac{PelPk}{AnkPk}\right] \times 100 \quad (2)$$

$$Shock\ attenuation^{torso}(\%) = \left[1 - \frac{HeadPk}{PelPk}\right] \times 100 \quad (3)$$

$$Shockattenuation^{body}(\%) = \left[1 - \frac{HeadPk}{AnkPk}\right] \times 100 \quad (4)$$

where *HeadPk* is the peak head acceleration, *PelPk* is the peak pelvis acceleration, and *AnkPk* is the peak tibia acceleration. All three shock attenuation indices were averaged between multiple stance phases (mean [SD] 43.16 [6.04]). An attenuation value of 0 indicates no attenuation, 100 indicates complete attenuation and a negative value indicates augmentation.

2.6.2. Frequency domain analysis

All analysis was performed in *Python v3.9* using the *SciPy v1.10* package. Unfiltered accelerometer signals were used for this analysis. Welch's method was used for Fast Fourier Transformation (Welch, 1967). The following parameters were used within the *scipy.signal.welch* function: fs = 400 – indicating the sampling frequency; detrend = "linear" – to detrend the time series signal; window = "boxcar"; nfft = 1024– to pad the signal with zeros to equal 1024 data points, ensuring periodicity (Shorten and Winslow, 1992). The power of all three accelerometer signals was quantified by calculating the power spectral density (PSD) of the frequencies between 0 and the Nyquist frequency (FN), and normalized to 1 Hz bins (Hamill et al., 1995). This resulted in the PSD having units of $g^2.Hz^{-1}$.

A transfer function (TF) was used to calculate signal power attenuation between the distal and proximal segments in decibels at each frequency interval using the following formula (Shorten and Winslow, 1992):

$$TF^{leg}_{low/high}(dB) = 10 \times log_{10}\left(\frac{PSD_{pelvis}}{PSD_{tibia}}\right) \quad (5)$$

$$TF^{torso}_{low/high}(dB) = 10 \times log_{10}\left(\frac{PSD_{head}}{PSD_{pelvis}}\right) \quad (6)$$

$$TF^{body}_{low/high}(dB) = 10 \times log_{10}\left(\frac{PSD_{head}}{PSD_{tibia}}\right) \quad (7)$$

where PSD_{head}, PSD_{pelvis}, and PSD_{tibia} are the power spectral densities (PSD) of the head, pelvis, and tibia resultant accelerations. TF was calculated across two signal frequency ranges: a lower (3–8 Hz) and a higher (9–20 Hz) frequency range (Fig. 2). The lower frequency range reflects the active motion of the body segment during running, whilst the higher frequency range reflects the impact-related shock-wave (Derrick et al., 1998). To align the directionality of the attenuation indices from the frequency- and time-domains, the TF value was multiplied by "−1". A positive TF value indicates a lower signal power at the proximal segment, compared to the distal segment – i.e. attenuation.

2.7. Statistical analyses

All statistical analyses were performed in R (v4.3.0), using the packages *correlation* (v0.8.4) for Bivariate Pearson correlations, *ncvreg* (3.14.1) for least absolute shrinkage and selection operator (LASSO) regression. All DEXA variables were assessed for Bivariate Pearson correlations against all shock (time-domain) and power (frequency-domain) attenuation variables. A statistically significant correlation was determined at an alpha of 0.05. Due to the exploratory nature of the study, no corrections were made for multiple comparisons. To determine the DEXA variables (eight predictors) that were most associative of each attenuation variable (nine outcomes), regularised regression was performed (Chowdhury and Turin, 2020). Prior to regression analysis, we centered all predictors to a mean of zero, so that the intercept has a

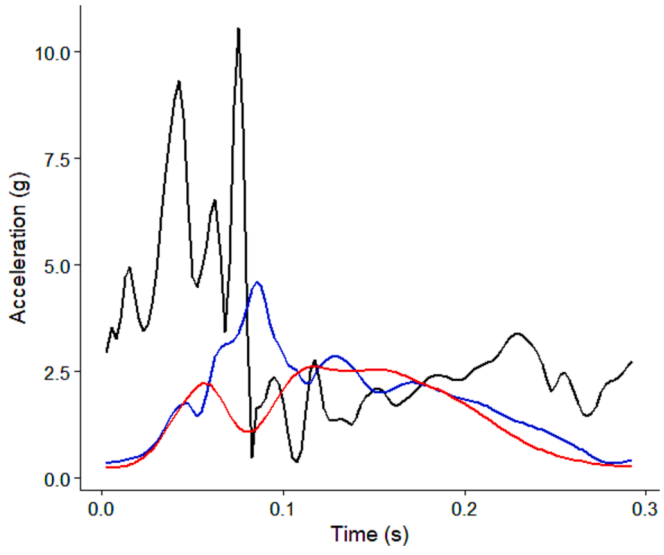

Fig. 1. A single participant trace over a single stance cycle of the resultant acceleration signal from the tibia (black), pelvis (blue), and head (red) sensors

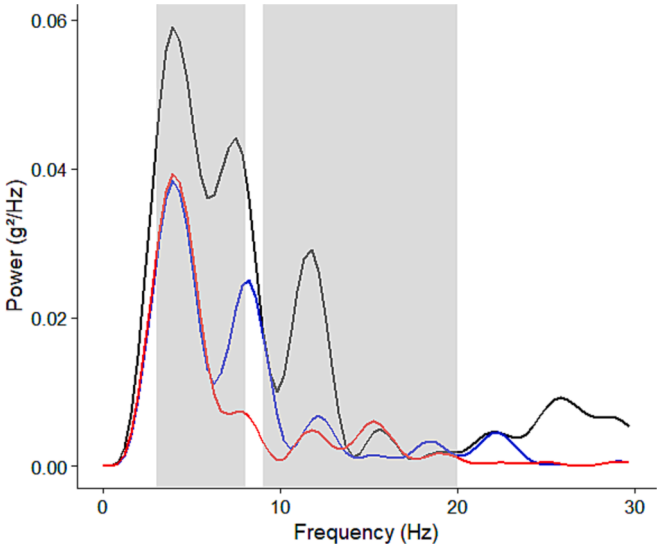

Fig. 2. A single participant power spectra from the tibia (black), pelvis (blue), and head (red) signals. Shaded boxes indicate the lower (3 to 8 Hz) and higher (9-20 Hz) ranges

meaningful interpretation. In the present study, we used the LASSO regression, which constitutes a penalized linear model with a shrinkage penalty that induces sparsity of predictors in the model (Moons et al., 2015; Tibshirani, 1996). Due to the L1-penalty used by the LASSO, the effects of predictors can be shrunk to zero, effectively resulting in predictor selection and thereby also improving prediction performance. The optimal amount of shrinkage induced by the algorithm is found via a 10-fold cross-validation (CV) (Tibshirani, 1996). For regularised regression, no p-values are produced.

3. Results

The descriptive demographic, running, and DEXA characteristics of participants are reported in Table 2, whilst characteristics of the accelerometry variables are in Table 3.

3.1. Tibia-pelvis

A greater attenuation between the tibia and pelvis was associated with a smaller trunk fat mass (−0.421, 95 %CI [−0.705, to −0.021], P = 0.041) (Fig. 3). For attenuation between the tibia and pelvis, the strongest predictor was trunk fat mass, where a 1 kg increase in mass predicted a 0.57 % reduction in attenuation (Table 4).

3.2. Pelvis-head

A greater power attenuation between the pelvis and head within the lower frequency range was associated with a greater trunk fat mass (0.468, 95 %CI [0.080, to 0.733], P = 0.021), leg fat mass (0.449, 95 % CI [0.056, to 0.722], P = 0.028), whole body fat mass (0.491, 95 %CI [0.109, to 0.746], P = 0.015), and visceral fat mass (0.449, 95 %CI [0.055, to 0.721], P = 0.028) (Fig. 3). A greater power attenuation between the pelvis and head within the higher frequency range was associated with a greater trunk fat-free mass (0.411, 95 %CI [0.009, to 0.698], P = 0.046), leg fat-free mass (0.524, 95 %CI [0.152, to 0.765], P = 0.009), and whole-body fat-free mass (0.480, 95 %CI [0.095, to 0.740], P = 0.018) (Fig. 3). A greater shock attenuation between the pelvis and head was associated with greater whole body fat mass (0.418, 95 %CI [0.017, to 0.703], P = 0.042) (Fig. 3).

For attenuation between the pelvis and head, the strongest predictor was leg fat mass, where a 1 kg increase in mass predicted a 2.14 % increase in attenuation (Table 4). For power attenuation of the high-frequency component between the pelvis and head, the strongest predictor was visceral fat mass, where a 1 kg increase in mass, resulted in a 48.79 dB increase in attenuation (Table 4). For power attenuation of the lower frequency component between the pelvis and head, the strongest predictor was whole-body fat mass, where a 1 kg increase in mass, resulted in a 1.50 dB increase in attenuation (Table 4).

3.3. Tibia-head

There were no shock indices that were significantly associated with the fat-free and fat mass (Fig. 3), and the latter DEXA variables also did not predict the shock indices in our regression analysis (Table 4).

4. Discussion

Shock attenuation is thought be associated with running injury risk potential and maintaining visual field stability. Our primary hypothesis was partially supported. A greater fat mass across the trunk, leg, and whole body was associated with greater power attenuation across the head and pelvis, in the lower frequency ranges (3–8 Hz) – i.e. attenuation of shock waves attributable to active movements. However, fat-free mass was associated with signal power attenuation across the head and pelvis, in the higher frequency ranges (9–20 Hz) – i.e. attenuation of shock waves attributable to impact. The strength of association between region-specific tissue composition and attenuation variables was similar to that for whole-body composition.

The relationship between fat-free mass and signal power attenuation in the higher frequency range, may suggest the importance of active muscular strategies in attenuating shock associated with the foot–ground collision during running. A previous study reported that landing with greater knee flexion resulted in greater power attenuation across

Table 2
Descriptive characteristics of participants.

Characteristic	N = 24[1]
Age (years)	25.0 (3.2)
Sex	
F	13/24 (54 %)
M	11/24 (46 %)
Body mass (kg)	61.83 (12.93)
Height (cm)	164.45 (11.35)
Body mass index (kg/m^2)	22.71 (3.62)
Leg dominance	
Right	24/24 (100 %)
Leg length (m)	0.83 (0.06)
Running experience (years)	
Below 1	10/23 (43 %)
1–2	7/23 (30 %)
2–3	2/23 (8.7 %)
3–5	2/23 (8.7 %)
5–10	1/23 (4.3 %)
10–20	1/23 (4.3 %)
Missing	1
Maximal running distance past 3 months in a single session	
Less than 5 km/Less than 3.2 miles	10/23 (43 %)
Between 5 and 15 km/between 3.2 and 9.6 miles	11/23 (48 %)
Between 15 and 25 km/between 9.6 and 15.9 miles	2/23 (8.7 %)
Missing	1
Running frequency	
Less than one time per week	1/21 (4.8 %)
1 time per week	2/21 (9.5 %)
2 times per week	8/21 (38 %)
3 times per week	6/21 (29 %)
4 times per week	3/21 (14 %)
7 times per week	1/21 (4.8 %)
Missing	3
Treadmill running speed (m/s)	2.86 (0.11)
Trunk fat mass (kg)	9.68 (3.72)
Trunk fat-free mass (kg)	18.33 (4.46)
Leg fat mass (kg)	3.98 (1.41)
Leg fat-free mass (kg)	6.58 (1.56)
Whole body fat mass (kg)	21.09 (7.15)
Whole body fat-free mass (kg)	39.20 (9.19)
Visceral fat mass (kg)	0.83 (0.36)
Visceral fat-free mass (kg)	1.50 (0.30)

[1] Mean (SD); n/N (%).

Table 3
Descriptive characteristics of accelerometry variables.

Variables	Mean (SD)
Peak tibia acceleration (g)	9.808 (5.355)
Peak pelvis acceleration (g)	5.464 (1.740)
Peak head acceleration (g)	2.762 (0.413)
Attenuation tibia-pelvis (%)	24.432 (38.833)
Attenuation tibia-head (%)	60.275 (19.314)
Attenuation pelvis-head (%)	44.352 (17.512)
Signal power magnitude tibia, high frequency ($g^2 \cdot Hz^{-1}$)	0.183 (0.223)
Signal power magnitude tibia, low frequency ($g^2 \cdot Hz^{-1}$)	0.285 (0.252)
Signal power magnitude pelvis, high frequency ($g^2 \cdot Hz^{-1}$)	0.084 (0.056)
Signal power magnitude pelvis, low frequency ($g^2 \cdot Hz^{-1}$)	0.140 (0.073)
Signal power magnitude head, high frequency($g^2 \cdot Hz^{-1}$)	0.027 (0.018)
Signal power magnitude head, low frequency($g^2 \cdot Hz^{-1}$)	0.067 (0.035)
Attenuation signal power pelvis-head, high frequency (dB)	121.757 (94.052)
Attenuation signal power tibia-head, high frequency (dB)	146.310 (176.263)
Attenuation signal power tibia-pelvis, high frequency (dB)	24.554 (169.505)
Attenuation signal power pelvis-head, low frequency (dB)	42.996 (31.186)
Attenuation signal power tibia-head, low frequency (dB)	68.664 (64.912)
Attenuation signal power tibia-pelvis, low frequency (dB)	25.668 (63.007)

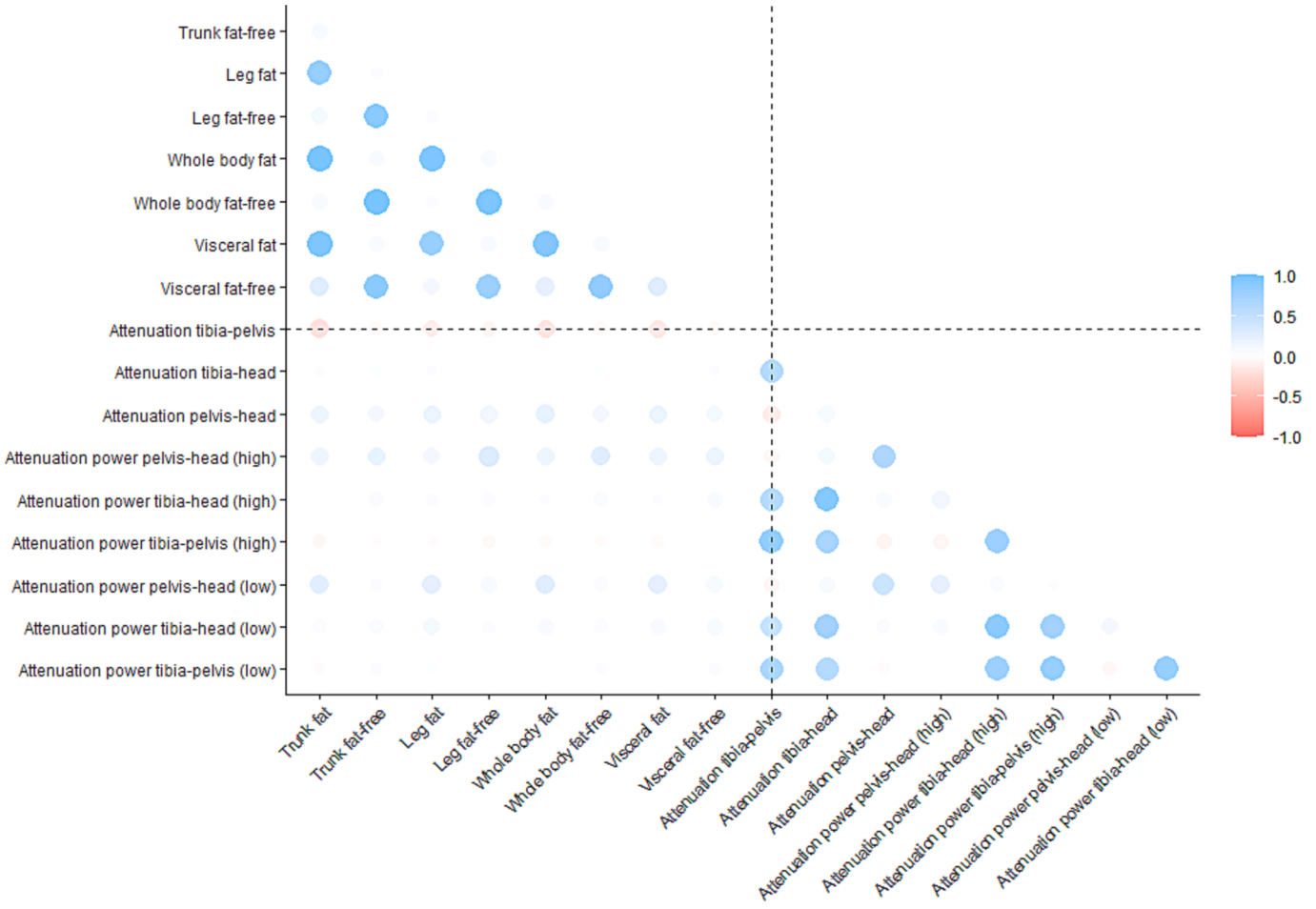

Fig. 3. Correlation matrix plot between DEXA and accelerometry variables

Table 4
Beta coefficients from LASSO regression of the DEXA predictors on each attenuation outcome variable. Blank cells indicate that variables were not selected.

Shock variables	Intercept	Trunk fat mass	Trunk fat-free mass	Leg fat mass	Leg fat-free mass	Whole body fat mass	Whole body fat-free mass	Visceral fat mass	Visceral fat-free mass
Tibia-pelvis attenuation	24.43	−0.57	–	–	–	–	–	–	–
Tibia-head attenuation	60.27	–	–	–	–	–	–	–	–
Pelvis-head attenuation	44.35	–	–	2.14	–	0.30	0.38	–	–
High frequency power attenuation pelvis-head	121.76	–	–	–	23.43	–	–	48.79	–
High frequency power attenuation tibia-head	146.31	–	–	–	–	–	–	–	–
High frequency power attenuation tibia-pelvis	24.55	–	–	–	–	–	–	–	–
Low frequency power attenuation pelvis-head	43.00	–	–	–	0.71	1.50	–	–	–
Low frequency power attenuation tibia-head	68.66	–	–	–	–	–	–	–	–
Low frequency power attenuation tibia-pelvis	25.67	–	–	–	–	–	–	–	–

the head and tibia in the higher frequency ranges of 10–35 Hz (Edwards et al., 2012). Landing with greater knee flexion requires greater knee and hip eccentric activity for energy absorption (Tamura et al., 2021; Zelik and Kuo, 2012), and so reflects a greater active muscular strategy, than landing with a more extended knee posture. One study reported that a greater percentage whole-body muscle mass, measured via bio-impedance, was associated with reduced axial tibial peak acceleration magnitude, and reduced signal power in the high (>10 Hz) frequency range (Giandolini et al., 2019). Associating fat-free mass with muscular strategies should be made with caution as the former also includes bone mass, and the latter rely on factors other than intrinsic anatomical form, such as motor control.

It has been suggested that the lower frequency ranges of shock reflect the acceleration caused by voluntary active movements (Derrick et al., 1998; Shorten and Winslow, 1992). If voluntary movement is closely associated with muscle mass, we should observe a lower correlation magnitude between fat-free mass and attenuation indices in the lower frequency ranges (<10 Hz). Yet, it is the fat mass indices which demonstrated the greatest correlation with attenuation of lower frequencies. One study reported that adult runners who were obese ran

with greater vertical stiffness than normal weight adults (Vincent et al., 2020). A greater vertical stiffness suggests a reduced vertical displacement during running, which may be a result of reduced lower-limb flexion, that increases shock attenuation (Zhang et al., 2008). Speculatively, a greater fat mass may result in smaller voluntary movements, potentially increasing vertical stiffness, and a reduced signal power attenuation of the lower frequency ranges.

Surprisingly, the strength of association between trunk fat/fat-free mass and signal power attenuation, was almost identical to the strength of association between whole body fat/fat-free mass and signal power attenuation. A previous study reported that whole-body fat percentage was not associated, but tibial fat and lean mass were associated with peak tibia acceleration (Schinkel-Ivy et al., 2012). The present study directly quantified local and global body composition via imaging, whereas the previous study relied on anthropometric measures and statistical equations to quantify body composition (Schinkel-Ivy et al., 2012). The similar association between local and global indices of fat/fat-free mass with power attenuation could be at least partly a result of the inclusion of participants within a relatively healthy weight range, where heterogeneity in relative fat distribution and body shapes are not observed. Local and global body composition indices may therefore be highly correlated in the present study (Fig. 3).

Findings from the present study could have implications for injury prevention and potentially the metabolic cost of running, which may influence the success of weight loss programs. For example, our regression analysis suggested the importance of fat-free leg mass on power attenuation of the high frequency components across the head and pelvis. This may be useful for recreational and/or elite athletes as it pertains to the management and prevention of back pain disorders (Maselli et al., 2020). In addition, our regression analysis revealed the association between visceral fat mass and signal power attenuation. This could mean that for individuals on a weight loss program, the greater the fat mass loss, the lesser it can contribute to signal power attenuation during running. Whether a reduction in fat mass increases injury risk during such a training program, and the trade-off it provides to other health benefits, needs to be investigated.

This study is not without limitations. First, we only recruited participants within a narrow and healthy body weight spectrum. Findings from this study should be generalised with caution to people who are overweight or obese. Also, the use and interpretation of shock attenuation determined from skin-mounted accelerometers on people with high adipose tissue mass should be done with caution. Skin-mounted accelerometers would be affected by soft-tissue artefacts, the magnitude of which depends on the placement of the sensors. A greater soft-tissue artefact would lead to a lower magnitude of time-domain, as well as low-frequency, shock variables (Lucas-Cuevas et al., 2017; Trama et al., 2021). Soft-tissue artefact may be more of an issue at the pelvis, than the distal tibia and the head. Second, our participants included a heterogenous spectrum of running experience. The relationship between body anthropometry and shock attenuation could be moderated by different running strategies, which itself could be influenced by running experience (Jiang et al., 2023). For example, different foot strike patterns affect shock attenuation magnitudes (Gruber et al., 2014), and the former may be influenced by running experience (Mo et al., 2023). Given that the present study did not quantify foot strike pattern, it may be that the relationship body anthropometry and shock attenuation could, in part, be explained by different running strategies. Third, whilst acknowledging the exploratory nature of the study, the large number of statistical analyses performed may still increase the false positive finding rate. As mitigation strategies, we did not deviate from our statistical plan, reported both significant and non-significant results, and used penalised regression methods. Hence, the findings presently should be considered within the hypothesis-generation framework.

5. Conclusions

Fat mass indices were mostly associated with attenuation of signal power between the pelvis and head in the lower frequency ranges, but fat-free mass indices were mostly associated with the same power attenuation in the higher frequency ranges. Greater fat-free mass appears to predict greater power attenuation capacity between the pelvis and head in the higher frequency ranges, which may benefit injury risk reduction. Depending on the location of the fat mass, reducing its mass may reduce power attenuation capacity, which could imply a greater injury risk potential during weight loss training programs.

Funding source: None.

CRediT authorship contribution statement

Bernard X.W. Liew: . **Xuqi Zhu:** Writing – review & editing, Writing – original draft, Visualization, Validation, Supervision, Software, Methodology, Formal analysis, Conceptualization. **Xiaojun Zhai:** Writing – review & editing, Writing – original draft, Validation, Supervision, Methodology, Formal analysis. **Stuart A. McErlain-Naylor:** Writing – review & editing, Writing – original draft, Visualization, Validation, Methodology, Investigation, Conceptualization. **Christopher McManus:** Writing – review & editing, Writing – original draft, Visualization, Validation, Supervision, Project administration, Methodology, Investigation, Formal analysis, Data curation, Conceptualization.

Declaration of competing interest

The authors declare that they have no known competing financial interests or personal relationships that could have appeared to influence the work reported in this paper.

Acknowledgements

We thank Joyal Jayan and Jerin Shaji for their efforts in collecting the data.

Appendix A. Supplementary data

Supplementary data to this article can be found online at https://doi.org/10.1016/j.jbiomech.2024.112025.

References

Baggaley, M., Vernillo, G., Martinez, A., Horvais, N., Giandolini, M., Millet, G.Y., Edwards, W.B., 2020. Step length and grade effects on energy absorption and impact attenuation in running. Eur. J. Sport Sci. 20, 756–766.

Bilsborough, J.C., Greenway, K., Opar, D., Livingstone, S., Cordy, J., Coutts, A.J., 2014. The accuracy and precision of DXA for assessing body composition in team sport athletes. J. Sports Sci. 32, 1821–1828.

Busa, M.A., Lim, J., van Emmerik, R.E.A., Hamill, J., 2016. Head and tibial acceleration as a function of stride frequency and visual feedback during running. PLoS One 11, e0157297.

Castillo, E.R., Lieberman, D.E., 2018. Shock attenuation in the human lumbar spine during walking and running. J. Exp. Biol. 221, jeb177949.

Chadefaux, D., Gueguen, N., Thouze, A., Rao, G., 2019. 3D propagation of the shock-induced vibrations through the whole lower-limb during running. J. Biomech. 96, 109343.

Chowdhury, M.Z.I., Turin, T.C., 2020. Variable selection strategies and its importance in clinical prediction modelling. Fam Med Community Health 8, e000262.

Derrick, T.R., Hamill, J., Caldwell, G.E., 1998. Energy absorption of impacts during running at various stride lengths. Med. Sci. Sports Exerc. 30, 128–135.

Edwards, W.B., Derrick, T.R., Hamill, J., 2012. Musculoskeletal attenuation of impact shock in response to knee angle manipulation. J. Appl. Biomech. 28, 502–510.

Enders, H., von Tscharner, V., Nigg, B.M., 2014. The effects of preferred and non-preferred running strike patterns on tissue vibration properties. J. Sci. Med. Sport 17, 218–222.

Fu, X.Y., Zelik, K.E., Board, W.J., Browning, R.C., Kuo, A.D., 2015. Soft tissue deformations contribute to the mechanics of walking in obese adults. Med. Sci. Sports Exerc. 47, 1435–1443.

Giandolini, M., Bartold, S., Horvais, N., 2019. Interaction between body composition and impact-related parameters in male and female heel-toe runners. Gait Posture 70, 355–360.
Gruber, A.H., Boyer, K.A., Derrick, T.R., Hamill, J., 2014. Impact shock frequency components and attenuation in rearfoot and forefoot running. J. Sport Health Sci. 3, 113–121.
Hamill, J., Derrick, T.R., Holt, K.G., 1995. Shock attenuation and stride frequency during running. Hum. Mov. Sci. 14, 45–60.
IAEA, 2011. Dual Energy X ray Absorptiometry for bone Mineral Density and Body Composition Assessment. International Atomic Energy Agency, Vienna.
Jiang, X., Xu, D., Fang, Y., Bíró, I., Baker, J.S., Gu, Y., 2023. PCA of running biomechanics after 5 km between novice and experienced runners. Bioengineering 10, 876.
Lucas-Cuevas, A.G., Encarnación-Martínez, A., Camacho-García, A., Llana-Belloch, S., Pérez-Soriano, P., 2017. The location of the tibial accelerometer does influence impact acceleration parameters during running. J. Sports Sci. 35, 1734–1738.
Maselli, F., Storari, L., Barbari, V., Colombi, A., Turolla, A., Gianola, S., Testa, M., 2020. Prevalence and incidence of low back pain among runners: a systematic review. BMC Musculoskelet. Disord. 21, 343.
Messier, S.P., Beavers, D.P., Loeser, R.F., Carr, J.J., Khajanchi, S., Legault, C., Devita, P., 2014. Knee joint loading in knee osteoarthritis: influence of abdominal and thigh fat. Med. Sci. Sports Exerc. 46, 1677–1683.
Mo, S., Huang, M., Ng, L., Cheung, R.T.H., 2023. Footstrike angle cut-off values to classify footstrike pattern in runners. Res. Sports Med. 31, 181–191.
Moons, K.G.M., Altman, D.G., Reitsma, J.B., Ioannidis, J.P.A., Macaskill, P., Steyerberg, E.W., Collins, G.S., 2015. Transparent reporting of a multivariable prediction model for individual prognosis or diagnosis (TRIPOD): explanation and elaboration. Ann. Intern. Med. 162, W1–W73.
Nana, A., Slater, G.J., Stewart, A.D., Burke, L.M., 2015. Methodology review: using dual-energy X-ray absorptiometry (DXA) for the assessment of body composition in athletes and active people. Int. J. Sport Nutr. Exerc. Metab. 25, 198–215.
Nielsen, R.Ø., Bertelsen, M.L., Ramskov, D., Damsted, C., Brund, R.K., Parner, E.T., Kjærgaard, S., 2019. The garmin-RUNSAFE running health study on the aetiology of running-related injuries: rationale and design of an 18-month prospective cohort study including runners worldwide. BMJ Open 9, e032627.
Pain, M.T.G., Challis, J.H., 2002. Soft tissue motion during impacts: their potential contributions to energy dissipation. J. Appl. Biomech. 18, 231–242.
Pain, M.T.G., Challis, J.H., 2006. The influence of soft tissue movement on ground reaction forces, joint torques and joint reaction forces in drop landings. J. Biomech. 39, 119–124.
Reenalda, J., Maartens, E., Buurke, J.H., Gruber, A.H., 2019. Kinematics and shock attenuation during a prolonged run on the athletic track as measured with inertial magnetic measurement units. Gait Posture 68, 155–160.
Schinkel-Ivy, A., Burkhart, T.A., Andrews, D.M., 2012. Leg tissue mass composition affects tibial acceleration response following impact. J. Appl. Biomech. 28, 29–40.
Sheerin, K.R., Reid, D., Besier, T.F., 2019. The measurement of tibial acceleration in runners – a review of the factors that can affect tibial acceleration during running and evidence-based guidelines for its use. Gait Posture 67, 12–24.
Shorten, M.R., Winslow, D.S., 1992. Spectral analysis of impact shock during running. Int. J. Sport Biomech. 8, 288–304.
Tamura, A., Akasaka, K., Otsudo, T., 2021. Contribution of lower extremity joints on energy absorption during soft landing. Int. J. Environ. Res. Public Health 18.
Tibshirani, R., 1996. Regression shrinkage and selection via the Lasso. J. R. Stat. Soc. Ser. B (Methodological) 58, 267–288.
Tirosh, O., Orland, G., Eliakim, A., Nemet, D., Steinberg, N., 2020. Attenuation of lower body acceleration in overweight and healthy-weight children during running. J. Appl. Biomech. 1–6.
Trama, R., Hautier, C.A., Souron, R., Lapole, T., Foure, A., Blache, Y., 2021. Is accelerometry an effective method to assess muscle vibrations in comparison to ultrafast ultrasonography? IEEE Trans. Biomed. Eng. 68, 1409–1416.
Villarrasa-Sapiña, I., Serra-Añó, P., Pardo-Ibáñez, A., Gonzalez, L.-M., García-Massó, X., 2017. Relationship between body composition and vertical ground reaction forces in obese children when walking. Clin. Biomech. (Bristol, Avon) 41, 77–81.
Vincent, H.K., Kilgore 3rd, J.E., Chen, C., Bruner, M., Horodyski, M., Vincent, K.R., 2020. Impact of body mass index on biomechanics of recreational runners. PM R 12, 1106–1112.
Wakeling, J.M., Liphardt, A.M., Nigg, B.M., 2003. Muscle activity reduces soft-tissue resonance at heel-strike during walking. J. Biomech. 36, 1761–1769.
Welch, P., 1967. The use of fast Fourier transform for the estimation of power spectra: a method based on time averaging over short, modified periodograms. IEEE Trans. Audio Electroacoust. 15, 70–73.
Zadpoor, A.A., Nikooyan, A.A., 2011. The relationship between lower-extremity stress fractures and the ground reaction force: a systematic review. Clin. Biomech. (Bristol, Avon) 26, 23–28.
Zelik, K.E., Kuo, A.D., 2012. Mechanical work as an indirect measure of subjective costs influencing human movement. PLoS One 7, e31143.
Zhang, S., Derrick, T.R., Evans, W., Yu, Y.J., 2008. Shock and impact reduction in moderate and strenuous landing activities. Sports Biomech. 7, 296–309.